

A Robust and Efficient Approach to License Plate Detection

Yule Yuan, *Member, IEEE*, Wenbin Zou, Yong Zhao, Xian Wang, Xuefeng Hu, and Nikos Komodakis

Abstract—This paper presents a robust and efficient method for license plate detection with the purpose of accurately localizing vehicle license plates from complex scenes in real time. A simple yet effective image downscaling method is first proposed to substantially accelerate license plate localization without sacrificing detection performance compared with that achieved using the original image. Furthermore, a novel line density filter approach is proposed to extract candidate regions, thereby significantly reducing the area to be analyzed for license plate localization. Moreover, a cascaded license plate classifier based on linear SVMs using color saliency features is introduced to identify the true license plate from among the candidate regions. For performance evaluation, a dataset consisting of 3828 images captured from diverse scenes under different conditions is also presented. Extensive experiments on the widely used Caltech license plate dataset and our newly introduced dataset demonstrate that the proposed approach substantially outperforms state-of-the-art methods in terms of both detection accuracy and run-time efficiency, increasing the detection ratio from 91.09% to 96.62% while decreasing the run time from 672 ms to 42 ms for processing an image with a resolution of 1082×728. The executable code and our collected dataset are publicly available.

Index Terms—license plate detection, line density transform, linear SVM, color saliency.

I. INTRODUCTION

INTELLIGENT transport systems play an important role in supporting smart cities because of their promising applications in various areas, such as electronic toll collection, highway surveillance, urban logistics and traffic management. One of the key components of intelligent transport systems is vehicle license plate recognition, which enables the identification of each vehicle by recognizing the characters on its license plate through various image processing and computer vision

Manuscript received Apr. 29, 2015; revised Sep. 3, 2015, Apr. 29, 2016, Oct. 11, 2016, and accepted Nov. 17, 2016. This work was supported in part by an NSFC project under Grant 61401287 and Grant 61472257, in part by the National Science Foundation of Shenzhen under Grant JCYJ20160506172651253 and Grant JCYJ20160307154003475, and in part by the Natural Science Foundation of SZU under Grant 2016058. The associate editor coordinating the review of this manuscript and approving it for publication was Dr. Quanzheng Li.

Y. Yuan is with School of Electronic and Computer Engineering, Peking University, Shenzhen 518055, China (e-mail: lemmas@foxmail.com).

W. Zou is with Shenzhen Key Lab of Advanced Telecommunication and Information Processing, the College of Information Engineering, Shenzhen University, Shenzhen 518060, China (e-mail: zouszu@sina.com).

Y. Zhao is the corresponding author. He is with the Key Laboratory of Integrated Microsystems, Peking University Shenzhen Graduate School, 518055, Shenzhen, China (e-mail: yongzhao@pkusz.edu.cn).

X. Wang is with the Key Laboratory of Integrated Microsystems, Peking University Shenzhen Graduate School, 518055, Shenzhen, China (e-mail: wangxa@pkusz.edu.cn).

N. Komodakis is with the LIGM Laboratory, École des Ponts ParisTech, Marne-la-Vallée 77455, France (e-mail: nikos.komodakis@enpc.fr).

techniques. Vehicle license plate recognition typically consists of license plate detection (LPD), character segmentation and recognition. LPD is the fundamental component of vehicle license plate recognition; as such, its performance, in terms of both detection accuracy and run-time efficiency, largely determines the overall accuracy and processing speed of the entire recognition system and thus influences the support provided for intelligent transport systems in smart cities.

The importance of LPD is well known in the computer vision community. A number of LPD methods have been proposed over the past two decades, and some of them have demonstrated success in certain specific tasks. However, as observed in [4], most of the previous methods perform well only under certain predefined conditions. Some common restrictions include fixed illumination, license plates with little blur or distortion from viewpoint changes, relatively simple backgrounds and the presence of only a single license plate in an image. More recent state-of-the-art approaches, e.g., [6][26][4], impose fewer restrictions on license plate detection at the cost of increased computational complexity. However, these approaches still have difficulty extracting license plates from complex scenes.

Considering the issues mentioned above, this paper develops an efficient and robust approach to license plate detection that is able to accurately localize one or multiple vehicle license plate(s) with diverse variations from complex backgrounds in real time. To speed up the detection algorithm overall, we first investigate how to reduce the size of the original high-resolution image without decreasing license plate detection performance. Note that because of the negative effects that are generally introduced by the downsampling method that is commonly used in image processing, most previously developed methods perform license plate detection using the original image. Then, we analyze the common characteristics among diverse license plates and their major differences with respect to background regions to serve as a basis for designing a region filter to exclude irrelevant regions in the image. Furthermore, we study which features are most discriminative for license plate detection and then propose an efficient and robust classifier to ultimately localize the exact position of the license plate in the image.

In summary, the contributions of this paper are as follows:

- 1) A novel line density filter (LDF) is proposed to extract candidate license plate regions, thereby significantly reducing the area to be analyzed for license plate localization.
- 2) An efficient license plate verification method is proposed to accurately detect the true license plate from among

the candidate regions using a cascaded license plate classifier (CLPC), which is trained based on color saliency features.

- 3) For performance evaluation, we present a newly collected challenging dataset that consists of 3828 license plate images with variations in illumination, license plate appearance, vehicle location and weather conditions.
- 4) We demonstrate that the proposed approach outperforms state-of-the-art methods by a large margin in terms of both detection accuracy and run-time efficiency.

This paper is organized as follows: In Section II, we briefly review the relevant literature on vehicle license plate detection. Section III introduces the proposed approach in detail. Experimental evaluations and discussions are presented in Section IV. Finally, Section V concludes the paper.

II. RELATED WORK

As the key step in a license plate recognition (LPR) system, LPD methods have made great strides in recent years [9] [10]. The following briefly reviews several LPD methods.

Based on the observation that vehicle license plates are characterized by abundant edge information, many methods exploit edge information for license plate detection. In [1], the magnitude of the vertical gradients is used to detect candidate license plate regions. Shapiro et al. [8] applied Robert's edge operator to emphasize vertical edges and used the projection of vertical edges to detect license plates. Zheng proposed a license plate extraction method [7] that searches for a license plate in a convolution output image using a rectangular shift window. Although this method is sensitive to window size, only a single license plate can be detected in any given image. Jia et al. [36] proposed a region-based method for LPD that uses the mean-shift approach to segment a color vehicle image and uses edge density information for license plate verification. Anagnostopoulos et al. [35] proposed an adaptive image segmentation technique to accelerate license plate detection. In [6], a block-based edge density prediction method was used to find candidate license plate regions, and a voting method based on multiple features was used for license plate verification. Although the detection step of this method is fast, its location accuracy primarily depends on the block size. Lalimi et al. [20] modified the region-based method of [36] and used morphological filtering to extract candidate regions. Ghaili et al. [13] proposed a vertical edge detection algorithm to speed up LPD methods. However, the improved computational efficiency is achieved at the cost of reduced edge information. In [37], edge clustering was exploited for license plate localization. Wang et al. [21] used gradient information and a trained cascade detection model for license plate detection.

The connection of character regions is another important cue for license plate extraction. Donoser et al. [12] proposed an LPD algorithm based on the maximally stable extremal region (MSER) concept [11], which enables the simultaneous localization and segmentation of individual characters. Li et al. [4] also used the MSER approach to detect character regions by exploiting bright and dark MSERs to handle all kinds

of Chinese license plates. These MSER-based methods can achieve high localization accuracy in relatively simple scenes. However, they have difficulty detecting character regions in more complex ones, e.g., scenes in which some areas of the license plate are contaminated.

The morphology technique [15], an important tool that is widely used in image processing tasks such as salient region detection [24] and object segmentation [31], has also been successfully applied for license plate detection by many authors. The morphology technique is typically used to detect the structural information of license plates. Hsieh et al. [17] used the differences between a 7×1 open operator and a 7×1 closed operator to locate license plates. In [5], a morphology gradient method for extracting license plate candidates was introduced that achieves an impressive average extraction ratio of 96.6%. However, the morphology technique is time consuming and is not suitable for license plate detection against complex backgrounds.

A number of previous approaches have extensively exploited color features for LPD, based on the observation that a license plate usually exhibits a regular color appearance of both its background and its characters. In [18], a neural network was applied to extract color features from the hue, saturation and lightness channels separately. Kim et al. [34] proposed combining color and texture features for the detection of license plates in images. In [23], Tian presented a license plate localization method based on a fixed color pair for the characters and background regions of a license plate. In [19], an edge-based and color-aided algorithm for license plate detection was proposed. Ashtari [38] introduced a method based on the modified template-matching technique for localizing an Iranian license plate in an image through an analysis of target color pixels. In this paper, we exploit color saliency and edge features for license plate detection.

III. THE PROPOSED APPROACH TO LICENSE PLATE DETECTION

This section presents our proposed approach to license plate detection, which consists of image preprocessing, candidate extraction and license plate verification. As illustrated in Fig. 1, the original color image is downscaled and converted into a grayscale image by the preprocessing procedure. Then, a set of candidate regions is extracted via edge density detection, adaptive thresholding for the detected edges and line density filtering. Finally, the license plate is located by verifying each of the candidate regions.

A. Image preprocessing

The original color images for license plate detection and recognition are generally captured at a high resolution (e.g., 1082×728), which ensures that the small license plates and the even smaller characters on them can be processed and recognized using computer vision algorithms. However, this high resolution also imposes a high computational cost for detecting the license plate in an image. To address this issue, one suggestion might be to downscale the input image for license plate detection. Unfortunately, the downscaling operation may

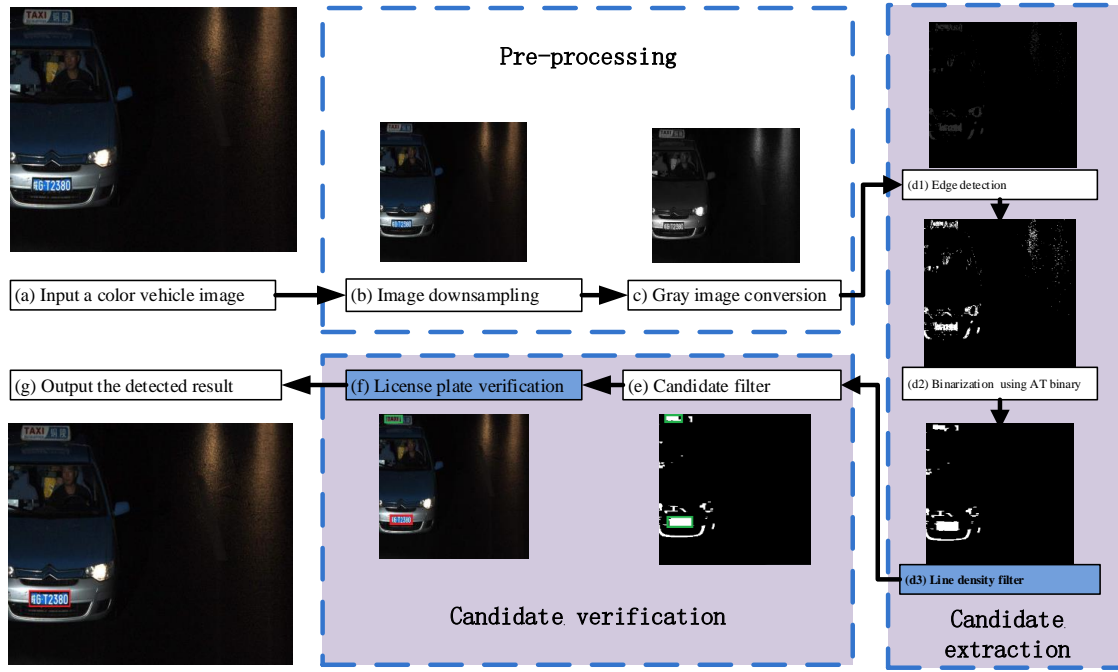


Fig. 1. Framework of the proposed license plate detection approach. The input color vehicle image is first processed via image downscaling and grayscale conversion. Then, a set of candidate regions for the target license plate is extracted through edge detection, binarization and line density filtering. Finally, the license plate is located by verifying the candidate regions using a cascaded license plate classifier.

result in a loss of information and lead to a decrease in license plate detection performance; for this reason, most previously developed methods do not perform image downscaling as part of the license plate detection task. Thus, a fundamental problem to be addressed is “how to balance detection accuracy and run-time efficiency for license plate detection”.

In this paper, we propose a novel image downscaling method for license plate detection that can substantially reduce the image size without incurring an obvious decrease in performance compared with that achieved when using the original image. This method is based on the following observations. First, the width of a license plate is obviously greater than its height. Second, the characters on a license plate are printed in the horizontal direction. Thus, we define different scale factors for the vertical and horizontal directions to downscale the original image, i.e.,

$$w_s = w_i/d_w \quad (1)$$

$$h_s = h_i/d_h \quad (2)$$

where w_i and h_i denote the width and height, respectively, of the original image, whereas w_s and h_s represent the corresponding downscaled dimensions, and d_w and d_h (s.t. $d_h < d_w$) are the downscaling factors for width and height, respectively. Note that a larger scale factor d_w should be assigned to downscale the original image in the horizontal direction for the following two reasons. First, we can compress more image data in the horizontal direction because the width of a license plate is obviously greater than its height. Second, a larger scale factor in the horizontal direction makes the characters on the license plate more compact, which allows the subsequently applied candidate region extraction method

to group all characters into a single region. In our experiments, d_w and d_h were set to 3 and 2, respectively. Using these well-defined scale factors, we exploit bilinear interpolation for image downscaling, in which each output pixel value is computed as a weighted average of the nearest pixels in a 2×2 neighborhood.

B. Candidate extraction using a line density filter

In this section, we propose a novel scheme for extracting license plate candidates. The candidate extraction method consists of edge detection, edge image binarization via adaptive thresholding (AT) and the proposed novel line density filter.

As illustrated in Fig.1, an extension of the Sobel operator is used to detect the boundaries of objects in the image. Then, AT [14] is exploited to eliminate weak edges and generate a binary edge image. Finally, a line density filter (LDF) method is proposed to connect the high-density regions in the binary edge image along the horizontal and vertical directions. Several examples of the results generated by each component of the candidate detection method are shown in Fig. 6. The following subsections describe the details of the proposed candidate extraction method.

1) Edge detection and density enhancement: For edge detection, we propose a simple extension of the Sobel operator for edge density enhancement. As illustrated in Fig. 2, p_0 denotes the current pixel, and p_1, p_2, p_3 , and p_4 are the nearest-neighbor pixels of p_0 . The edge intensity e_0 for pixel p_0 is defined as follows:

$$e_0 = \begin{cases} \Gamma & \text{if } d_0 \geq \Gamma \\ d_0 & \text{else } d_0 < \Gamma \end{cases} \quad (3)$$

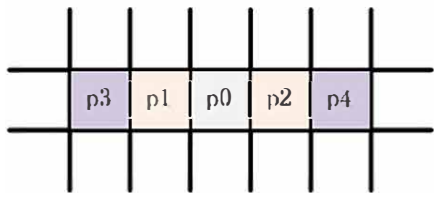


Fig. 2. The edge intensity for the current pixel p_0 is computed from the nearest-neighbor pixels p_1, p_2, p_3 and p_4 .

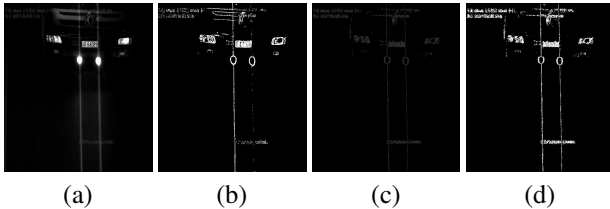


Fig. 3. Edge detection results generated by the Sobel operator and by our proposed method: (a) grayscale input image, (b) edge detection result obtained using the Sobel operator, (c) edge detection result obtained using the proposed extension of the Sobel operator, and (d) the result of applying adaptive thresholding to (c).

where Γ is a defined threshold value and d_0 is computed as

$$d_0 = |p_1 + p_2 - 2 \times p_0| + |p_3 + p_4 - 2 \times p_0| \quad (4)$$

Compared with the typical Sobel operator, which uses a pair of 1×3 (or 3×3) convolution masks to estimate the gradient in the vertical and horizontal directions, we use a single 1×5 mask to estimate the gradient in the vertical direction only. Experimentally, we have found that a 1×5 convolution mask is more robust for edge detection than a 1×3 mask. The threshold value Γ was set to 48 in our experiments to avoid overflow in the hardware implementation of the subsequent adaptive thresholding operation. An example of the edge detection results generated by the Sobel operator and by our proposed method is presented for visual comparison in Fig. 3.

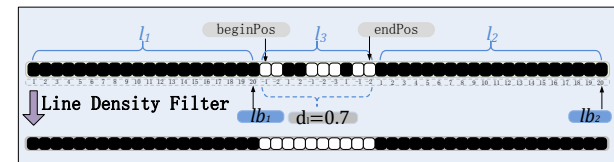
2) *Adaptive thresholding*: To further enhance the estimated edges and generate a binary edge image E_b , we perform adaptive thresholding (AT) [14] on the previously generated grayscale edge image E_g . Given E_g , the AT method generates an integral image E_i by summing all pixel values from the upper left corner for each pixel in E_g . Then, a binary edge image E_b is generated by thresholding each pixel $p(x, y)$ in the integral image E_i using a threshold that is adaptively computed from a local window in E_i . Specifically, $E_b(x, y)$ is computed as follows:

$$E_b(x, y) = \begin{cases} 255 & \text{if } E_i(x, y) \geq \beta \varpi(x, y) \\ 0 & \text{else } E_i(x, y) < \beta \varpi(x, y) \end{cases} \quad (5)$$

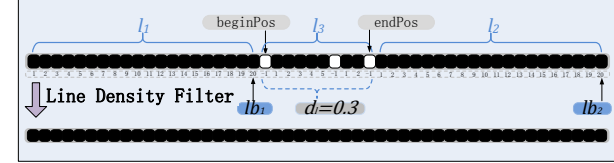
where β is the coefficient used to control the threshold and $\varpi(x, y)$ is the average of all pixel values within the local $h_w \times h_w$ window surrounding pixel $p(x, y)$, i.e.,

$$\varpi(x, y) = \frac{1}{h_w \times h_w} \sum_{\substack{-h_w/2 < k < h_w/2 \\ -h_w/2 < j < h_w/2}} E_i(x+k, y+j) \quad (6)$$

In our experiments, the parameters β and h_w were set to 0.7 and 20, respectively.



(a)



(b)

Fig. 4. An illustration of the LDF processing of two rows in an image, where lb_1 and lb_2 represent the lengths of line segments l_1 and l_2 , respectively. For illustration, the line density threshold is taken to be 0.4. The high-density line segment l_3 in (a) is connected (in white) by the LDF, whereas the lower-density one in (b) is removed (in black).

3) *Line density filer*: Given the edge image generated via AT, we attempt to highlight the license plate area and remove noise in the binary image. The morphology technique is typically used as a mathematical tool to address such problems in image processing. Wu et al. [5] presented an impressive morphology gradient method for detecting license plates. Bai et al. [25] introduced a hybrid method using edge statistics and morphology to extract license plate regions. However, the conventional morphology filter is very time-consuming because its template usually contains several pixels, which increases the computational cost. Thus, this filter may not be appropriate for applications that require real-time processing. Therefore, we propose an efficient line density filter (LDF) to highlight the character region.

Our proposed LDF approach is motivated by the following observations:

- 1) License plates generally exhibit a relatively high edge density.
- 2) The characters on a license plate are printed in a horizontal orientation, and the height of each character is nearly identical.
- 3) If an image contains multiple license plates, some spatial distance will exist between each of them.

The underlying concept of the LDF is to, by observing the abovementioned cues, connect regions of high edge density and remove sparse regions in each row and column in the binary edge image E_b . An illustration of the LDF processing of two rows in an image is shown in Fig. 4, where non-edge pixels are shown in black and edge pixels are shown in white. Suppose that l_1 and l_2 represent two continuous black line segments, with lengths of lb_1 and lb_2 pixels, respectively. The target line segment l_3 , which contains both edge pixels and non-edge pixels, is the one for which we wish to either connect or remove the white edge pixels. We make this decision based on the line density d_l , which is defined as the proportion of edge pixels in the line segment l_3 , i.e.,

$$d_l = \frac{w_l}{w_l + b_l} \quad (7)$$

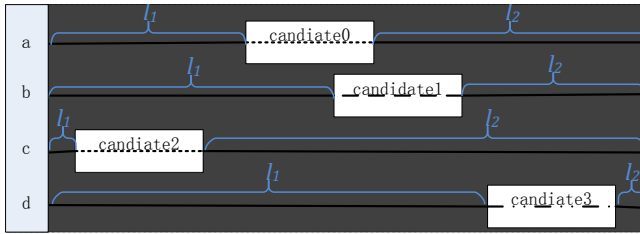


Fig. 5. Candidate license plate locations in four lines. The lengths of line segments l_1 and l_2 are lb_1 and lb_2 , respectively. Candidate 0 and candidate 1 are located in the middle of the image, such that $lb_1 > T_{min}$ and $lb_2 > T_{min}$. Candidate 2 is close to the leftmost side of the image, such that $lb_1 < T_{min}$ and $lb_2 > T_{min}$. Candidate 3 located near the rightmost boundary of the image, such that $lb_1 > T_{min}$ and $lb_2 < T_{min}$.

where w_l and b_l denote the numbers of white and black pixels, respectively, in the line segment l_3 .

Ideally, we suppose that non-plate areas exist on both sides of the license plate. In other words, there should be relatively long black line segments (e.g., l_1 and l_2) on both sides of a discontinuous line segment (e.g., l_3) to be processed. To find such a relationship between the line segments l_1 , l_2 and l_3 , we propose the following scheme for calculating the lengths of the line segments. A black pixel is counted as 1, whereas a white pixel is counted as -1. If continuous black pixels exist, we group them together. Similarly, if continuous white pixels exist, we calculate the cumulative length of each white line segment, which is represented by a negative number. Several examples of the length calculation for horizontal lines are shown in Fig. 4. The length calculation for vertical lines is the same but in the vertical direction.

Using the generated horizontal line-length map for each pixel of the binary image, we apply the proposed LDF to extract the license plate candidates. The pseudocode for our horizontal line density filter (HLDF) is presented in Algorithm 1. This pseudocode contains four input parameters: the binary image E_b ; the minimum length threshold for a black line, T_{min} , for l_1 or l_2 ; the gap-length threshold, T_{gap} , for l_3 (between l_1 and l_2); and the line density threshold T_{d_l} for l_3 . The default values for T_{min} , T_{gap} and T_{d_l} were set to 20, 8 and 0.05, respectively, in our experiments. Note that as a special case, the candidate may be located too close to the left or right image boundary, that is, the leftmost line segment l_1 or the rightmost line segment l_2 may have a length of less than T_{min} ; in this case, the algorithm should reapply the same processing to l_3 . In Fig. 5, the top two lines illustrate condition C1 as denoted in Algorithm 1, whereas the bottom two lines represent conditions C2 and C3, which require reprocessing.

For the vertical direction, we can apply the same pseudocode to the transposed binary image E_b . For the vertical line density filter (VLDF), the parameters T_{min} , T_{gap} , and T_{d_l} were set to 10, 6 and 0.03, respectively, in our experiments. Fig. 6 shows several candidate license plate regions processed using the LDF method to demonstrate the robustness of our LDF algorithm under different illumination conditions.

Algorithm 1 Horizontal Line Density Filter

```

INPUT: image  $E_b$  and thresholds  $T_{min}$ ,  $T_{gap}$ , and  $T_{d_l}$ 
OUTPUT: image  $E_b'$ 
Calculate the horizontal length map  $M_{hl}$  from binary image  $E_b$ 
for each line in length map  $M_{hl}$  do
    Find two line segments  $l_1$  and  $l_2$ , with lengths of  $lb_1$  and  $lb_2$ , respectively
    C1 =  $lb_1 > T_{min}$  and  $lb_2 > T_{min}$ 
    C2 =  $l_1$  is the leftmost line segment and  $lb_1 < T_{min}$  and  $lb_2 \geq T_{min}$ 
    C3 =  $l_2$  is the rightmost line segment and  $lb_1 \geq T_{min}$  and  $lb_2 < T_{min}$ 
    if C1 or C2 or C3 then
        Calculate  $d_l$  for line  $l_3$ 
        if  $d_l \geq T_{d_l}$  then
            Set all pixels of  $l_3$  to white in  $E_b'$ 
        else
            Set all pixels of  $l_3$  to black in  $E_b'$ 
        end if
    end if
end for

%the following pseudocode is for removing minor white noise
for each line in  $M_{hl}$  do
    if  $lb_1 \geq T_{min}$  and  $lb_2 \geq T_{min}$  then
        horGap =  $endPos - beginPos + 1$ 
        if  $horGap < T_{gap}$  then
            Fill all pixels of  $l_3$  with black in  $E_b'$ 
        end if
    end if
end for

```

C. Candidate extraction via CCL

Once the candidate regions have been obtained using the LDF method, we need to further distinguish the true license plate region(s) from other regions. We use a two-step approach to verify these candidate regions. First, connected-component labeling (CCL) is applied to find candidates and remove areas that obviously do not exhibit the geometrical characteristics of a license plate, which are defined as 1) $24 < w < 256$, 2) $6 < h < 32$, 3) $256 < w * h < 4096$, and 4) $w/h < 6$, where w and h represent the width and height, respectively, of the labeled rectangle. These parameters were chosen based on the minimum and maximum widths and heights of a wide range of possible license plates to cover the potential characteristics of most scenes, and they can be modified to be suitable for license plates in different countries or administrative regions.

D. Verification via a CLPC based on color saliency

The final step of LPD is to identify the real license plates from among the detected candidate regions. Li et al. [4] constructed a conditional random field model (CRF) to find the final license plates. In [21], a cascade AdaBoost classifier was proposed to verify candidates. Other methods for license plate verification include principal visual word discovery [26] and CNNs [27]. In [18], a neural network (NN) was trained based on the HSL color space to determine whether each pixel belonged to a license plate region. Wang et al. [33] proposed a fuzzy logic method for license plate recognition.

Considering that a license plate usually consists of two dominant colors, we propose a cascaded license plate classifier (CLPC) based on linear SVMs [2] using color saliency features to verify license plate candidates, inspired by [16] [28]. The feature vector is extracted from both the HSV and RGB color spaces to ensure the effectiveness of the CLPC.

To eliminate the negative impact of illuminate variations and decrease the computational complexity of license plate verification, a quantization scheme for color feature representation



Fig. 6. Vehicle images and their license plate candidate results generated by the proposed LDF algorithm, where the bottom two examples are from our dataset and the others are from the Caltech dataset: (a) original grayscale source images, (b) results of edge density detection and enhancement, (c) binary images obtained via adaptive thresholding (AT), and (d) candidate results generated by our line density filter (LDF).

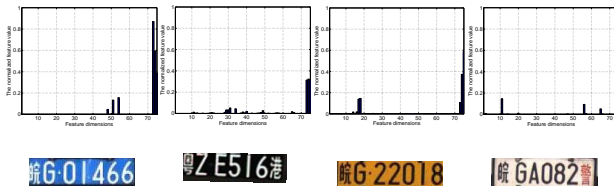


Fig. 7. Color histograms for various types of license plates.

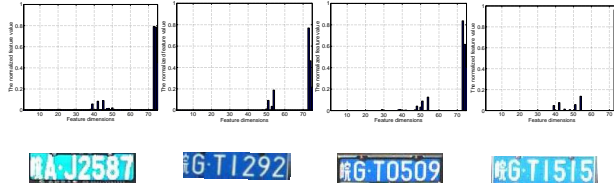


Fig. 8. Color histograms for blue license plates under different lighting conditions.

is needed. In the HSV color space, the hue, saturation, and value channels are quantized into 8, 3 and 3 bins, respectively, thereby generating a 72-dimensional ($8 \times 3 \times 3$) color feature vector. For each color level $c \in [0, 72]$, we obtain a saliency value $S(c)$ as follows:

$$S(c) = \frac{\sum_{x=\frac{2cw}{3}, y=ch}^{x=\frac{2cw}{3}, y=ch} \omega(p(x, y)) == c}{ch \times cw/3} \quad (8)$$

where ω represents the quantization processing and cw and ch denote the width and height, respectively, of a candidate region. The HSV color space alone is insufficient to achieve the desired classification results. Therefore, the mean values $\bar{\varphi}_i$ for the individual R, G and B channels are also included in the feature vector; these values are calculated as follows:

$$\bar{\varphi}_i = \frac{\sum_{x=\frac{2cw}{3}, y=ch}^{x=\frac{2cw}{3}, y=ch} \varphi_i(x, y)}{255 \times ch \times cw/3}, i \in \{R, G, B\} \quad (9)$$

where φ represents the color value in each of the RGB channels. By cascading the 72-dimensional HSV feature vector into the 3 RGB color values, each candidate region can be represented by a 75-dimensional feature vector.

Fig. 7 shows the color histograms for various types of license plates. As observed from this figure, the color histograms for different types of license plates are markedly different. Fig. 8 shows the color histograms for blue license plates under different lighting conditions. Surprisingly, these color histograms are quite similar despite the diverse illumination of the license plates, which demonstrates the robustness of the proposed feature representation.

Although the feature vector can be efficiently computed using this quantization scheme, the quantization itself may introduce artifacts. For instance, some similar colors may be quantized into different bins. To reduce the noise introduced by the quantization, we use the smoothing method suggested in [28], i.e.,

$$S'(c) = \frac{1}{(m-1)T} \sum_{i=1}^m ((T - D(c, c_i))S(c_i)) \quad (10)$$

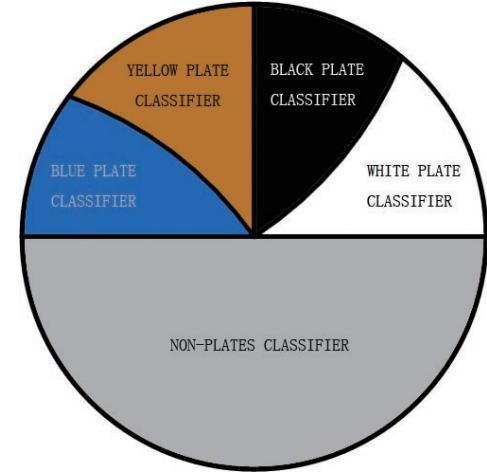


Fig. 9. The CLPC trained using linear SVMs. If a candidate does not belong to the set {blue license plate, yellow license plate, black license plate, white license plate}, it is considered a non-plate region.

where $D(c, c_i)$ is a metric representing the color distance between pixels c and c_i and $T = \sum_{i=1}^m D(c, c_i)$ is the sum of the distances between color c and its m nearest neighbors c_i . The normalization factor arises from $\sum_{i=1}^m (T - D(c, c_i)) = (m-1)T$.

In contrast to the conventional methods, in which a binary classifier is trained to categorize a region as either a license plate region or not, here we propose a cascaded license plate classifier (CLPC) that consists of four sub-classifiers based on four different types of Chinese license plates: blue license plates, black license plates, yellow license plates, and white license plates. Fig. 9 illustrates the construction of the CLPC. The decision function for determining whether a candidate is a license plate region or a non-plate region can be described in set notation as follows: $\{c \in \text{non-plate} \mid c \notin \{ \text{blue license plate, black license plate, yellow license plate, white license plate} \}\}$.

The advantages of the proposed CLPC are twofold. On the one hand, the CLPC is theoretically able to provide an improved classification accuracy compared with conventional classifiers. For example, if the error rate of each sub-classifier is 10%, then the total error rate of the CLPC is $0.1^4 = 0.0001$. In practice, this mechanism can achieve a classification accuracy of 98.9% on our dataset. On the other hand, the CLPC is also very fast because it uses simple linear SVMs. To train the CLPC, we randomly selected 200 license plate region images for each type of plate as positive samples and 3000 non-plate region images as negative samples.

IV. EXPERIMENTAL EVALUATION

Our LPD algorithm was implemented in C++ on a PC with a 3.2 GHz dual-core CPU and 4 GB of RAM. The proposed approach was extensively evaluated on the widely used Caltech vehicle dataset and our newly collected dataset. The executable code and our dataset are publicly available¹.

In this section, the two datasets used for performance evaluation are introduced first. Then, we compare our approach

¹www.wzou.eu

TABLE I
DESCRIPTIONS OF OUR PKU AND CALTECH VEHICLE DATASETS.

Dataset	Scene description	Resolution	Image quantity	Plate quantity	Plate height (pixels)
PKU G1	Cars on highways; normal environment during daytime; one license plate	1082×728	810	810	35-57
PKU G2	Cars and trucks on highways; daytime with sunshine glare; one license plate	1082×728	700	700	30-62
PKU G3	Cars and trucks on highways; nighttime; one license plate	1082×728	743	743	29-53
PKU G4	Cars and trucks on city roads; daytime with reflective glare; one license plate	1600×1236	572	572	30-58
PKU G5	Cars and trucks at intersections with crosswalks; multiple license plates	1600×1200	1152	1438	20-60
Caltech	Cars in diverse outdoor scenes; one plate per image	896×592	126	126	23-59

TABLE II
EXPERIMENTAL CONDITIONS.

Scenes	highway toll stations, urban roadsides, intersections
Weather	sunny, shady, rainy
Time	daytime and nighttime
Camera specs	14 fps
Camera distance to vehicle	5-15 m
Camera placement	pan + 25°, tilt 15°
License plate sizes	diverse sizes
License plate design	single row
Vehicle colors	diverse colors

TABLE III
DETECTION RATIOS (AS PERCENTAGES) FOR THE VARIOUS METHODS ON THE PKU (G1-G5) AND CALTECH VEHICLE DATASETS.

Method	G1	G2	G3	G4	G5	Caltech	Average
Zheng [7]	94.93	95.71	91.91	69.58	67.61	77.8	82.92
Zhao [6]	95.18	95.71	95.13	69.93	68.10	85.7	84.96
Zhou [26]	95.43	97.85	94.21	81.23	82.37	84.8	89.32
Li [4]	98.89	98.42	95.83	81.17	83.31	88.9	91.09
Our approach	98.76	98.42	97.72	96.23	97.32	91.27	96.62

with various state-of-the-art methods [6] [7] [26] [4] in terms of both detection accuracy and run-time efficiency. Afterward, we analyze the impact of image downscaling factors on the performance of the LPD algorithm. Finally, we present several failure cases of license plate detection and analyze the reasons for failure.

A. Datasets

To evaluate the performance of our proposed LPD algorithm in a wide range of intelligent transport scenarios, we performed experiments on the public Caltech vehicle dataset and also collected a dataset of 3828 vehicle images to further validate the robustness of our proposed approach. Several vehicle images and their license plate detection results are shown in Fig. 13 and Fig. 14.

We first used the Caltech vehicle dataset [29] to evaluate the license plate detection performance. This dataset includes 126 images captured from complex outdoor scenes during the day, each of which contains only a single vehicle, i.e., only one license plate exists in each vehicle image.

Considering the limitations of the Caltech vehicle dataset, we collected a new dataset, called the PKU vehicle dataset, for license plate detection performance evaluation. Our collected PKU dataset includes 3828 vehicle images captured from various scenes under diverse conditions. As shown in Table I, we categorize our vehicle images into five groups (i.e., G1-G5) corresponding to different configurations. For example, the images in G1 were captured on highways during the daytime under normal conditions, and each image in G1 contains only a single car; by contrast, the images in G5 were captured at intersections with crosswalks during either the day or night, and each image in G5 contains multiple license plates, some of which have defects. The experimental conditions for the collection of the PKU vehicle images are summarized in Table II.

B. Detection ratio

To evaluate license plate detection performance in terms of localization accuracy, we assume that each license plate is totally encompassed by the bounding box and that $c \cap t / c \cup t \geq 0.5$ [32], where c is the detected candidate region (indicated by red rectangles in this paper) and t is the ground-truth license plate region. The experimental detection results for the five tested methods on the two datasets are shown in Table III. As seen from this table, Li's method [4] achieves slightly a higher detection ratio on the relatively simple PKU G1 dataset, in which none of the license plates are blurred or affected by defects. However, it does not perform well when the license plates are contaminated by soil, such as in some images in G4 and G5. One reason is that when characters on a license plate are obscured, the MSER method used in [4] is not able to detect character regions correctly. The other reason is that some of the license plates in G4 are interrupted by reflective glare and some of the images in G5 include multiple license plates, and these conditions lead to detection failure in the MSER method. The other methods considered for comparison also have difficulty detecting multiple license plates in an image. Quantitatively, our method achieves detection ratios of 97.69% and 91.27% on the PKU dataset (G1-G5) and the Caltech dataset, respectively. On average, our proposed approach achieves a 96.62% detection ratio and a 5.53% improvement compared with the best of the reference methods.

It is interesting to see the impact of using different thresholds for edge detection in our approach on the overall license plate detection performance. As shown in Fig. 10, the detection ratio increases with an increasing threshold Γ when the threshold is set to relatively small values, whereas the detection performance remains relatively stable when Γ is within the range of [48, 56]. Therefore, Γ was set to 48 in all experiments.

C. Localization recall and precision

To evaluate our method more objectively, we computed the precision and recall of the various methods of license plate

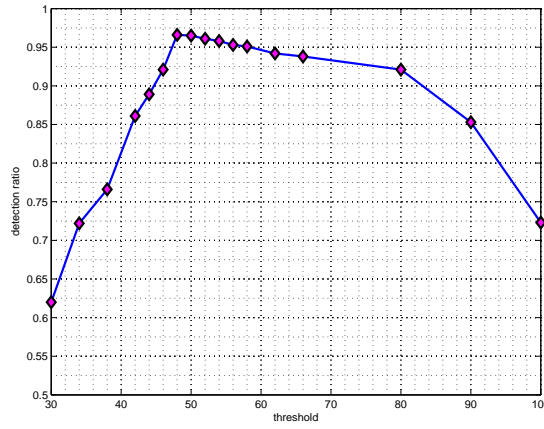


Fig. 10. Detection ratios achieved using different thresholds Γ in Eq. (3) for edge detection.

detection for various values of the matching confidence ξ between the predicted bounding box c and the ground truth t , inspired by [30] [32]. The matching confidence ξ is defined as follows:

$$\xi = \{c \cap t / c \cup t \mid t \subseteq c\} \quad (11)$$

For a given matching confidence ($\xi = \xi_0$), the precision and recall are defined as follows:

$$Precision = TP / (TP + FP) \quad (12)$$

$$Recall = TP / (TP + FN) \quad (13)$$

where TP and FP denote the numbers of correctly and incorrectly detected license plates, respectively, and FN denotes the number of license plates that failed to be detected.

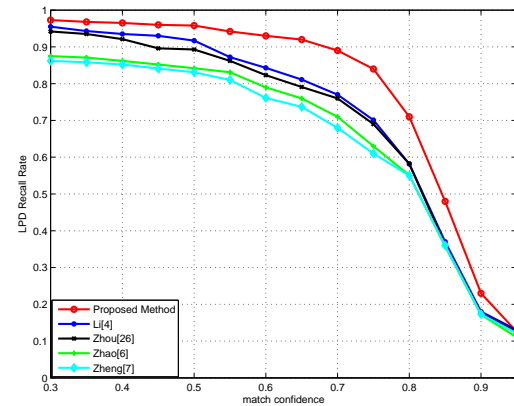
Fig. 11 presents the precision and recall results for various matching confidence values ξ . As observed from this figure, Li's method is slightly superior in terms of precision when the matching confidence is greater than 0.8. However, our proposed approach achieves an obviously higher recall throughout the entire range of matching confidence values.

D. Run time

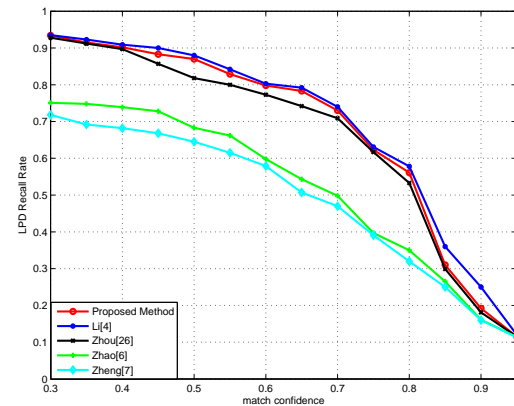
Table IV presents the average run times of our proposed approach and the other state-of-the-art methods for processing a high-resolution image (1082×728). As seen from this table, our approach is the fastest, requiring only 42 ms for license plate detection, whereas Li's method, which ranks second in terms of detection performance in Table III, requires 672 ms. Therefore, our proposed approach is robust and efficient. Table V shows the average run time for each step of our approach. Clearly, the most time-consuming step is the image downscaling, which should thus be considered the highest priority for further optimization.

E. Image downscaling validation

To validate our proposed image downscaling algorithm for license plate detection, we report the detection ratios and run times of our proposed method that are achieved using the original input image and the corresponding downscaled image.



(a) Recall



(b) Precision

Fig. 11. Recall and precision of different methods by using various matching confidence (ξ) values.

TABLE IV
AVERAGE RUN TIMES OF THE DIFFERENT METHODS FOR PROCESSING AN IMAGE WITH A RESOLUTION OF 1082×728 .

License plate detection algorithm	Average time (ms)
Zheng [7]	357
Zhao [6]	183
Zhou [26]	475
Li [4]	672
Proposed	42

TABLE V
AVERAGE RUN TIMES FOR EACH STEP OF THE PROPOSED METHOD FOR PROCESSING IMAGES OF DIFFERENT RESOLUTIONS.

Algorithm step	1082 \times 728 resolution	1600 \times 1236 resolution
Image downscaling	18 ms	34 ms
Grayscale	7 ms	13 ms
Edge detection + AT+ LDF	12 ms	28 ms
CCL	2 ms	4 ms
CLPC	3 ms	4 ms
Total time	42 ms	83 ms

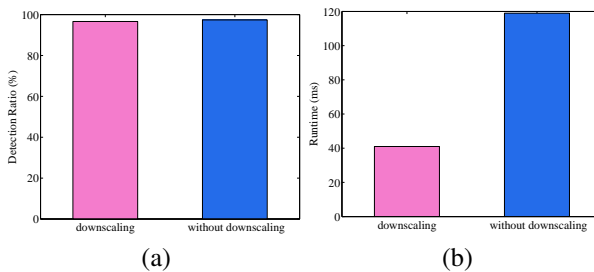


Fig. 12. LPD performance in terms of detection ratio (a) and run time (b) of the proposed approach using the original input image and the corresponding downsampled image.

As seen in Fig. 12, the image downscaling operation does not lead to any obvious decrease in performance compared with that achieved when using the original high-resolution image for license plate detection. However, it substantially decreases the overall run time of our approach, from 118 ms to 42 ms, which is the purpose of performing image downscaling for license plate detection.

F. Qualitative analysis

Fig. 13 and Fig. 14 show several examples of detection results generated by our proposed approach. We can draw several observations from these examples. First, for images that contain a single license plate in a normal environment, such as those in Fig. 13, our approach exactly locates the license plates with very few candidate regions (indicated by red and green bounding boxes). Second, for images that contain multiple license plates against a complex background and or under weak illumination, such as those in the third row of Fig. 14, the proposed method may generate additional candidate regions; however, it is able to exclude the irrelevant ones and ultimately locate the true license plates, as indicated by the red bounding boxes.

Nevertheless, our proposed approach may fail on certain difficult scenes. Fig. 15 presents the typical failure cases. For images with reflective glare on the license plates, such as the example presented in the first row, most of the edges of the license plate are not extracted during adaptive thresholding and, thus, the license plate is not found among the candidate regions. When the neighborhood of the license plate contains false characters (e.g., the second example), the candidate region is too large, which leads to verification failure.

V. CONCLUSION AND FUTURE WORK

This paper presents a novel and efficient approach to license plate detection (LPD). The proposed approach consists of three components: image preprocessing, candidate extraction and license plate verification. A simple yet effective image downscaling method is proposed for use in the image preprocessing step; this method is able to substantially decrease the run-time complexity of license plate localization without sacrificing detection accuracy compared with that achieved using the original image. To extract candidate license plate regions from the downsampled image, an extension of the Sobel operator is proposed for detecting the boundaries of objects

in the image. Furthermore, a line density filter (LDF) that connects high-edge-density regions and removes noise in each row and column as well as a postprocessing operator are proposed for candidate extraction. Finally, a cascaded license plate classifier (CLPC), which is trained using color saliency features, is proposed to detect the true license plate(s) from among the candidate regions by cascading multiple linear support vector machines. For performance evaluation, a new dataset is presented that contains 3828 images captured under diverse conditions and in diverse environments. The proposed approach was extensively evaluated on both the widely used Caltech license plate dataset and our new dataset (the PKU license plate dataset). The experiments demonstrated that our proposed approach substantially outperforms state-of-the-art methods in terms of detection accuracy and run-time efficiency, increasing the detection ratio from 91.09% to 96.62% while decreasing the run time from 672 ms to 42 ms for the processing of an image with a resolution of 1082×728.

As demonstrated in the experiments, the proposed approach and the other state-of-the-art methods are all still subject to certain limitations when addressing difficult scenes, e.g., reflective glare on license plates. In the future, it would be interesting to exploit the MSER or Hough transform approach to address such difficult cases.

ACKNOWLEDGMENT

Yule Yuan and Wenbin Zou contributed equally to this paper and are co-first authors.

The authors would like to thank the anonymous reviewers and the Associate Editor, Dr. Quanzheng Li, for their insightful comments and suggestions, which have been greatly beneficial for improving the quality of this paper. The authors also thank Jin Fang, Peijun Tang, and Siying He for their assistance with the dataset collection.

REFERENCES

- [1] S. Wang, H. Lee, "Detection and recognition of license plate characters with different appearances," in Proc. IEEE Conf. Intell. Transp. Syst. (ITSC), vol.2, pp.979-984, (2003).
- [2] R. E. Fan, K. W. Chang, C. J. hsieh, X. R. Wang, C. J. Lin, "LIBLINEAR: A Library for Large Linear Classification," *Journal of Machine Learning Research*, vol.9, pp.1871-1874, (2008).
- [3] A. Rosenfeld, J. Pfaltz, "Sequential operations in digital picture processing," *J. ACM*, vol. 13, no. 4, pp. 471-494, (1996).
- [4] B. Li, B. Tian, Y. Li, D. Wen, "Component-based license plate detection using conditional random field model," *IEEE Trans. Intell. Transp. Syst.*, vol.14, no.4, pp.1690-1699, (2013).
- [5] H. H. Wu, H. H. Chen, R. J. Wu, D. F. Shen, "License plate extracion in low resolution video," in Proc. IEEE Int. Conf. Pattern Recognit. (ICPR), Hong Kong, pp.824-827, (2006).
- [6] Y. Zhao, Y. L. Yuan, S. B. Bai, K. Liu, W. Fang, "Voting-based license plate location," in Proc. IEEE Conf. Intell. Transp. Syst. (ITSC), pp.314-317, (2011).
- [7] D. Zheng, Y. Zhao and J. Wang, "An efficient method of license plate location," *Pattern Recognit. Lett.*, vol.26, no.15, pp.2431-2438, (2005).
- [8] V. Shapiro, G. Gluhchev, D. Dimov, "Towards a multinational car license plate recognition system," *Mach. Vis. Appl.*, vol.17, pp.173-183, (2006).
- [9] C. N. E. Anagnostopoulos; I. E. Anagnostopoulos; I. D. Psoroulas; V. Loumos; E. Kayafas, "License Plate Recognition From Still Images and Video Sequences: A Survey," *IEEE Trans. Intell. Transp. Syst.*, vol.9, iss.3 pp.377-391, (2008).
- [10] D. Shan, M. Ibrahim, M. Shehata, W. Badawy, "Automatic license plate Recognition (ALPR): A State-of-the-Art Review," *IEEE Trans. Circuits Syst. Video Technol.*, vol.23, no. 2, pp.311-324, (2013).



Fig. 13. Examples of detection results generated by the proposed LPD approach on the Caltech dataset [29]. The red and green bounding boxes represent the detected candidate regions; the red ones correspond to the final detected license plates.

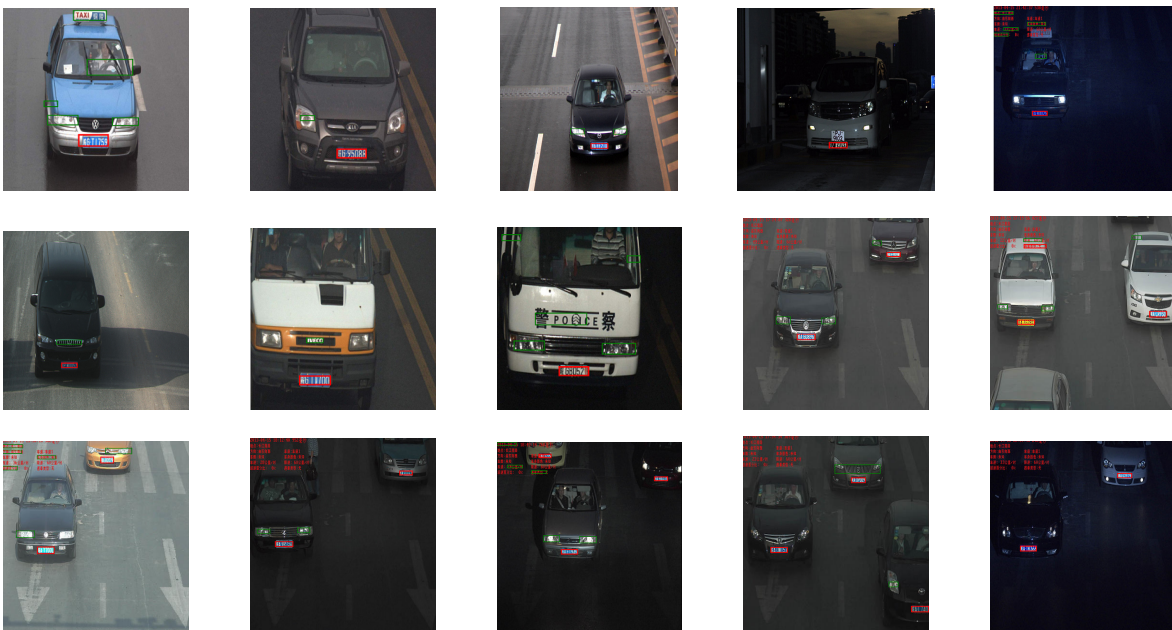


Fig. 14. Examples of detection results generated by the proposed LPD approach on our PKU vehicle dataset. The red and green bounding boxes represent the detected candidate regions; the red ones correspond to the final detected license plates.

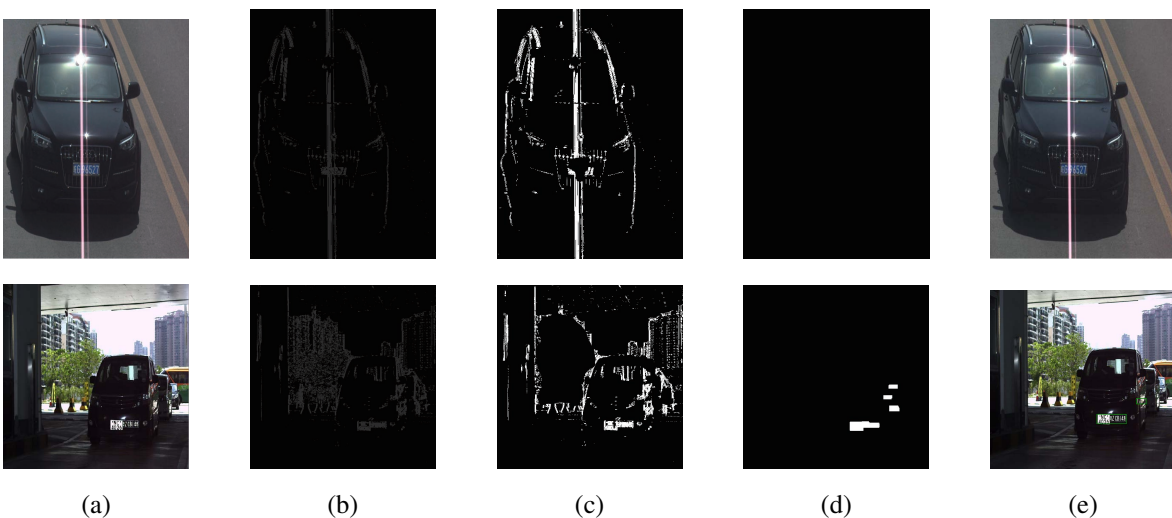


Fig. 15. Two examples of failed detection: (a) downsampled color input images, (b) results of edge density detection and enhancement, (c) binary edge images obtained via adaptive thresholding (AT), (d) candidate results generated by our line density filter (LDF), (e) results verified by the CLPC, where the red and green bounding boxes represent the detected candidate regions, with the red ones corresponding to the final detected license plates.

- [11] J. Matas, O. Chum, M. Urban, and T. Pajdla, "Robust wide baseline stereo from maximally stable extremal regions", *Image Vis. Comput.*, vol.22, no.10, pp.761-767, (2004).
- [12] M. Donoser, C. Arth, H. Bischof, "Detecting, tracking and recognizing license plates," *In Proc. Aisian Conf. Comput. Vis. (ACCV)*, pp.447-456, Springer, (2007).
- [13] A.M. Al.Ghaili, S. Mashohor, A. R. Ramli, A. Ismail, "Vertical-Edge-Based Car-License-Plate Detection Method," *IEEE trans. veh. technol.*, vol.62, no.1, (2013).
- [14] D. Bradley, G. Roth, "Adaptive thresholding using the integral image," *J. Graph. Tools*, vol.12, no.2, pp.13-21, (2007).
- [15] R. M. Haralick, S. R. Sternberg, and X. Zhuang, "Image analysis using mathematical morphology," *IEEE Trans. Pattern Anal. Mach. Intell.*, vol.4, pp.532-550, (1987).
- [16] W. Zou, Z. Liu, K. Kpalma, J. Ronsin, Y. Zhao and N. Komodakis, "Unsupervised Joint Salient Region Detection and Object Segmentation," *IEEE Trans. Image Process.*, vol. 24, no. 11, pp. 3858-3873, (2015).
- [17] J. W. Hsieh, S. H. Yu, Y. S. Chen, "Morphology-based license plate detection from complex scenes," *in Proc. Int. Conf. Pattern Recognit. (ICPR)*, Quebec City, Canada, pp.176-179, (2002).
- [18] E. R. Lee, P. K. Kim, H. J. Kim, "Automatic recognition of a car license plate using color image processing," *in Proc. IEEE Int. Conf. Image Process. (ICIP)*, pp.301-305, (1994).
- [19] V. Abolghasemi, A. Ahmadyfard, "An edge-based color-aided method for license plate detection," *Image and Vis. Comput.*, vol.27, pp.1134-1142, (2009).
- [20] M. A. Lalimi, S. Ghofrani, D. McLernon, "A vehicle license plate detection method using region and edge based methods," *Computers and Electrical Engineering*, vol.39, pp.834-845, (2013).
- [21] R. Wang, N. Sang, R. Huang, Y. Wang, "License plate detection using gradient information and cascade detecors", *Optik*, vol.125, pp.186-190, (2014).
- [22] X. Shi, W. Zhao, Y. Shen, "Automatic license plate recognition system based on color image processing", *Lecture Notes on Computer Science*, vol. 3483, Springer, New York, pp. 1159-1168, (2005).
- [23] J. Tian, R. Wang, G. Wang, and F. Yang, "A new algorithm for license plate localization in open environment using color pair and stroke width features of character", *In Proc. Int. Symposium on Multispectral Image Process. and Pattern Recognit.*, pp.892117, (2013).
- [24] Liu, Z., W. Zou, and M. O. Le. "Saliency tree: a novel saliency detection framework." *IEEE Trans. Image Process.*, vol. 23.5,1937-52 (2014).
- [25] H. Bai, and C. Liu, "A hybrid license plate extraction method based on edge statistics and morphology", *in Proc. Int. Conf. Pattern Recognit. (ICPR)*, Cambridge, U.K., pp.831-834, (2004).
- [26] W. Zhou, H. Li, Y. Lu, Q. Tian, "Principal visual word discovery for automatic license plate detection," *IEEE Trans. Image Process.*, vol.21, no.9, pp.4269-4279, (2012).
- [27] Y. N. Chen, C. C. Han, C. T. Wang, B. S. Jeng, K. C. Fan, "The application of a convolution neural network on face and license plate detection," *in Proc. Int. Conf. Pattern Recognit. (ICPR)*, vol.3, pp.552-555, (2006).
- [28] M. M. Cheng, G. X. Zhang, N. J. Mitra, X. Huang, S. M. Hu, "Global contrast based salient region detection," *in Proc. IEEE Comput. Vis. Pattern Recognit. (CVPR)*, pp.409-416, (2011).
- [29] Caltech Plate Dataset. (2003) [Online]. Available: http://www.vision.caltech.edu/Image_Datasets/cars_markus/cars_markus.tar
- [30] B. Epshtain, E. Ofek, and Y. Wexler, "Detecting text in natural scenes with stroke width transform," *in Proc. IEEE Comput. Vis. Pattern Recognit. (CVPR)*, pp.2963-2970, (2010).
- [31] W. Zou, C. Bai, K. Kpalma and J. Ronsin, "Online Glocal Transfer for Automatic Figure-Ground Segmentation," *IEEE Trans. on Image Process.*, vol. 23, no. 5, pp. 2109-2121, (2014).
- [32] K. Lin, H. tang, and T.S. Huang, "Robust license plate detection using image saliency," *in Proc. Int. Conf. Pattern Recognit. (ICPR)*, Sep. 2010, pp.3945-3948. (2010).
- [33] F. Wang, L. Man, B. Wang, Y. Xiao, W. Pan, and X. Lu, "Fuzzy-based algorithm for color recognition of license plates," *Pattern Recognit. Lett.*, vol.29, no.7, pp.1007-1020, (2008).
- [34] K. I. Kim, K. Jung, J. H. Kim, S. W. Lee, and A. Verri, "Color texture based object detection: An application to license plate localization," *in Lecture Notes on Computer Science*, Berlin, Germany: Springer-Verlag, vol. 2388, pp. 293-309, (2008).
- [35] C. N. E. Anagnostopoulos, I. E. Anagnostopoulos, V. Loumos, E. Kayafas, "A License Plate-Recognition Algorithm for Intelligent Transportation System Applications," *IEEE Trans. Intell. Transp. Syst.*, vol.7,pp.377-392, (2006).
- [36] W.J. Jia, H.F. Zhang, X.J. He, "Region-based license plate detection," *J. Network Comput. Appl.*, vol.30, pp.1324-1333, (2007).
- [37] G.S. Hsu, J.-C. Chen, and Yu-Zu Chung, "Application-Oriented License Plate Recognition," *IEEE Trans. Veh. Technol.*, vol.62,no.2,pp.552-561, (2013).
- [38] A. H. Ashtari, M. J. Nordin, and M. Fathy, "An Iranian License Plate Recognition System Based on Color Features," *IEEE Trans. Intell. Transp. Syst.*, vol.15, no.4, pp.1690-1704, (2014).



Yule Yuan received his undergraduate degree in Computer Science from Three Gorges University, Yichang, China, in 2000. He received an M.E. degree in Software Engineering from Peking University, Beijing, China, in 2008. He is currently a candidate for a Ph.D. degree in Electrical and Computer Engineering at Peking University. From 2001 to 2004, he was a senior software engineer at e-Future Information Technology Inc. From 2008 to 2009, he was an engineer at C2 Microsystems, Beijing, China. From 2009 to 2011, he worked as a research engineer at Shenzhen Graduate School of Peking University, Shenzhen, China. His research interests and areas of publication include image processing, video analysis, and machine learning.



Wenbin Zou received a Ph.D. degree from the National Institute of Applied Sciences (INSA), Rennes, France, in 2014. He received an M.E. degree in Software Engineering, with a specialization in Multimedia Technology, from Peking University, China, in 2010. He was a Visiting Research Student with the Hong Kong University of Science and Technology from 2008 to 2009. He is currently with the faculty of the College of Information Engineering, Shenzhen University, China. He is also a Post-doctoral Fellow with the UMR Laboratoire d'Informatique Gaspard-Monge, CNRS, and the École des Ponts ParisTech, France. His current research interests include saliency detection, object segmentation, and semantic segmentation.



Yong Zhao received a B.S. degree in Mathematics from Guizhou University, Guiyang, China, in 1985; an M.E. degree from Northwestern Polytechnic University, Xi'an, China, in 1988; and a Ph.D. degree in Engineering from the Research Institute of Automation, Southeast University, Nanjing, China, in 1991. From 1991 to 1994, he worked as a research assistant in the Department of Biomedical Engineering at Zhejiang University. From 1994 to 1997, he worked as a vice dean/associate professor in the Department of Electrical Engineering at Hanzhou University (now Zhejiang University). From 1997 to 2000, he worked as a post-doctoral fellow in the Center for Signal Processing and Communications, Electrical and Computer Engineering at Concordia University, Montreal, Canada. From 2000 to 2004, he worked as a senior software engineer at Honeywell Corporation, Ottawa, Canada. Since 2004, he has been with Shenzhen Graduate School of Peking University, Shenzhen, China, where he is currently an associate professor. His research interests and areas of publication include video codecs, signal processing, and machine learning.



Xuefeng Hu received a B.S. degree from Beijing Information Technology Institute, Beijing, China, in 2004 and an M.S. degree from Peking University, Beijing, China, in 2007. From 2007 to 2010, he worked as a software engineer at the China Electric Power Research Institute and Beijing C2 Microsystems. He is currently a Ph.D. candidate at Peking University. His research interests include computer vision and image processing.



Xinan Wang received a B.S. degree in Computer Science from Wuhan University, Wuhan, China, in 1983 and M.S. and Ph.D. degrees in Microelectronics from Shanxi Microelectronics Institute, Xian, China, in 1989 and 1992, respectively. He is currently a Professor with the School of Electronics Engineering and Computer Science at Peking University, Beijing, China. He is now working at the School of Electronic and Computer Engineering, Peking University, Shenzhen Campus. His research interests are focused on the areas of application-specific integrated-circuit design and IC design methodology.



Nikos Komodakis is currently an Associate Professor with the Université Paris-Est and the École des Ponts ParisTech and is a Research Scientist with the UMR Laboratoire d'Informatique Gaspard-Monge, CNRS. He is also an affiliated Adjunct Professor with the École Normale Supérieure de Cachan. His research interests lie in the areas of computer vision, image processing, machine learning, and medical imaging, and he has authored numerous papers in the above domains for many prestigious journals and conferences. He serves on the Editorial Board of the *International Journal of Computer Vision* and as an Associate Editor of *Computer Vision and Image Understanding*.